

DOI: 10.1515/amm-2017-0051

D. BOLIBRUCHOVÁ<sup>\*#</sup>, L. RICHTÁRECH<sup>\*</sup>, S.M. DOBOSZ<sup>\*\*</sup>, K. MAJOR-GABRYŚ<sup>\*\*</sup>

## UTILISATION OF MOULD TEMPERATURE CHANGE IN ELIMINATING THE $Al_5FeSi$ PHASES IN SECONDARY $AlSi7Mg0.3$ ALLOY

This article describes the impact of the metal mould temperature change in eliminating the adverse effect of iron in the  $AlSi7Mg0.3$  alloy. The kind of phases based on iron to be formed in aluminium alloys is determined by the alloy chemical composition, the melt overheating temperature prior to casting, and the cooling rate during crystallisation. In the experiment, we used three various mould temperatures, and their impact on the possible change in the adverse  $Al_5FeSi$  phase, excreted in a needle form to a more compact form of Chinese writing or skeleton units. The experimental part did not use melt overheat that would result in impairment of the melt, for example due to increased gassing of the melt, as well as in a greater load on the smelting unit, thus resulting in increased energy expenditure. We can conclude from the obtained results that the mould temperature change does not have an adequate effect in eliminating the adverse effect of iron in Al-Si-Mg alloys.

*Keywords:*  $AlSi7Mg0.3$  alloy, correctors of iron, recycled materials, Iron based intermetallic phase, thermal analysis

### 1. Introduction

Iron is generally considered the most problematic impurity in aluminium alloys. Iron has a very low solubility in a solid aluminium solution (max. 0.05 wt. %). Together with other additive elements (especially silicon, manganese, chromium and copper) it hence produces intermetallic phases that significantly reduce mechanical properties of the castings, particularly their ductility. These intermetallic phases are very brittle, their Young's elasticity module and thermal expansion coefficient are significantly different from those of the  $\alpha$ -Al solid solution matrix. Therefore, these phases apply as significant tension concentrators in mechanical stress [1,2]. The worst effects on mechanical properties of aluminium alloys are exercised by phases with board-like morphology and the currently often discussed polyedric morphology phases. Therefore, we are still looking for ways of preventing the above-mentioned phases to occur in castings. Partial reduction of negative properties of the above-mentioned intermetallic phases in gravity cast aluminium alloys with relatively low iron content is carried out by simply modifying the chemical composition of the melt, adding other elements that ensure transformation of the board-like morphology into a more compact shape of, for example, the "Chinese writing". The additive elements that reduce the adverse effect of iron in aluminium alloys by changing the morphology of phases based on iron include mainly Mn, Cr, Co, Mo, Ni, Be or rare earth metals (REM) [1,3,4]. The possibility of using sedimen-

tation process to reduce iron content in aluminium alloys has already been dealt with in the works that deal with the creation of polycomponent intermetallic phases with high iron content, which started to manifest negatively for example in the process of casting aluminium alloys under pressure [5-7]. The phases are typically referred to as sludge phases. They are of polyedric or branched nature. These phases may achieve dimensions on the order of centimetres in holding furnaces. Of course, the presence of such phases in castings inevitably means a significant reduction in strength and ductility [8-10]. Due to their high hardness, problems often occur even with possible machining of the castings. Therefore the above-mentioned problems forced manufacturers to solve this issue. We can use casting thermal treatment to influence crystallisation germs, which includes significant melt overheating above the melt liquidus temperature and utilisation of different cooling rates during casting [11-13].

### 2. Experiment

The purpose of the experiment was to verify the possibilities of influencing, by temperature change of the mould, the morphology of adverse ferrous phases in an  $AlSi7Mg0.3$  alloy with higher iron content. As an experimental material, we used the  $AlSi7Mg0.3$  alloy with high iron content during the experiment. The chemical composition of the used alloy is shown in Table 1. All the melting processes were performed at the melt temperature

\* DEPARTMENT OF TECHNOLOGICAL ENGINEERING, FACULTY OF MECHANICAL ENGINEERING, UNIVERSITY OF ŽILINA, UNIVERZITNÁ 1, 010 26, SLOVAK REPUBLIC

\*\* AGH UNIVERSITY OF SCIENCE AND TECHNOLOGY, FACULTY OF FOUNDRY ENGINEERING, 30 MICKIEWICZA AL., 30-059 KRAKÓW, POLSKA

# Corresponding author: Danka.Bolibruchova@fstroj.uniza.sk

of  $760 \pm 5^\circ\text{C}$ . The melt was gravity cast into a metal mould. The melt was not inoculated, modified or degassed in the melting processes. Prior to casting, only the oxide layer was removed from the surface. During casting, three different mould temperatures were used:  $100^\circ\text{C} \pm 5^\circ\text{C}$ ,  $150^\circ\text{C} \pm 5^\circ\text{C}$  and  $200^\circ\text{C} \pm 5^\circ\text{C}$ .

TABLE 1

Chemical composition of AlSi7Mg0.3 with higher iron content

Element	Si	Fe	Cu	Mn	Mg	Ni
[wt. %]	6.49	<b>1.280</b>	0.053	0.092	0.349	0.034
Element	Cr	Pb	Ti	Zn	Sb	
[wt. %]	0.087	0.006	0.113	0.027	<0.0004	

The effect of the mould temperature change on the microstructure and shape of excreted phases was detected using black-and-white contrast. Sample preparation and the microstructure images were carried out using a standard method of evaluating intermetallic phases in aluminium alloys. We used  $\text{H}_2\text{SO}_4 + \text{H}_2\text{O}$  solution as etchant. Microstructure images from individual samples were obtained using a light microscope. In Figure 1 we can see the impact of mould temperature on the microstructure of the AlSi7Mg0.3 secondary alloy. It is obvious that the mould temperature had a significant influence on the formation of phases in the alloy. At the mould temperature of  $100^\circ\text{C}$ , the structure

excretes long particles of  $\beta$ -phase ( $\text{Al}_3\text{FeSi}$ ), wherein with increasing temperature these particles are significantly shortened and the structure is dominated by phases in the shape of the so-called “Chinese writing” or skeletal formations. EDX analysis of the skeletal formations from Figure 1c is shown in Figure 2.

EDX analysis confirmed the presence of elements Al (69 wt. %), Si (9 wt. %), Fe (20 wt. %) and Mn (2 wt. %). According to the chemical composition, the phases thus had the character of a board-like  $\beta$ -phase, with negligible manganese content.

Adding iron correctors is a commonly used method, since they allow changing the shape of board-like formations of the  $\text{Al}_3\text{FeSi}$  phase (brittle form) into a globular shape or the so-called “Chinese writing” shape (less brittle form). Mn is a commonly used corrector in alloys of the Al-Si type. The correction effect is attributed also to Cr, V and Ni.

In complex elimination of iron in the given secondary alloy together with the mould temperature change we used as correctors chromium in the form of AlCr20 master alloy and nickel in the form of AlNi20 master alloy in three tiered amounts (0.5; 1 and 1.5 wt. %). Simultaneously with the added corrector we measured thermal analyses of individual melting processes that were to verify the effect of adding correctors on the creation of new phases in the alloy. The measurement results from the thermal analyses can be seen in Figures 3 and 4.

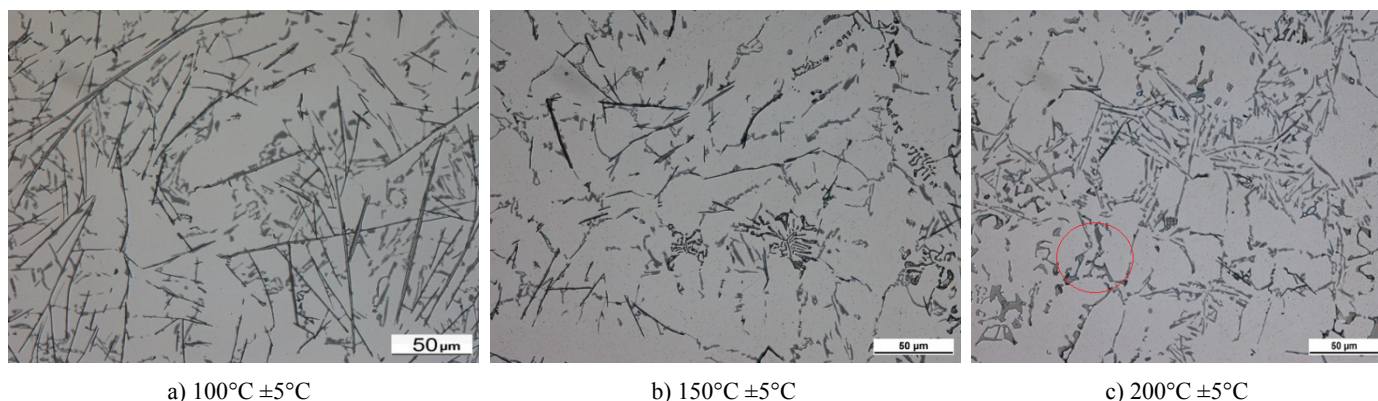
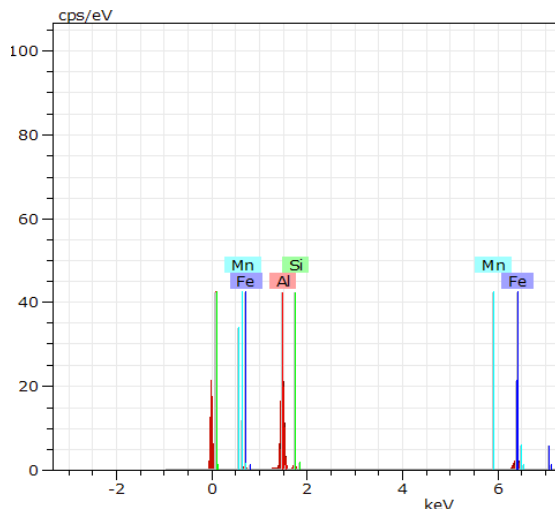
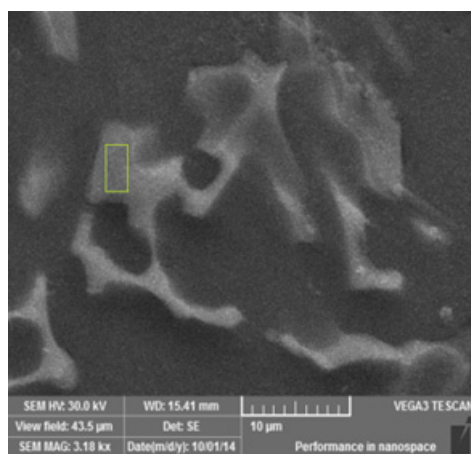


Fig. 1. Microstructure of AlSi7Mg0.3 secondary alloy with different mould temperatures

Fig. 2. EDX analysis of the skeletal phase of AlSi7Mg0.3 secondary alloy at the mould temperature of  $200^\circ\text{C}$

We can conclude from the thermal analysis results that the addition of master alloy to a higher iron content alloy reduces the liquidus temperature and increases the solidus temperature. Both master alloys also increase the time of eutectic reaction, which is given by the effect of releasing latent heat generated in the crystallisation of new phases. Figure 5 shows images of microstructures with different mould temperatures after adding 0.5 wt. % of AlCr20.

Figure 5 clearly shows that the structure features various types of phases, independent of the mould temperature. Figures 5a and 5b show clusters of sludge phases as well as clusters of board-like  $\beta$ -phases. The mould temperature impact on the structure after adding 1 wt. % of AlCr20 is shown in Figure 6.

The microstructure images show that after the ingot mould temperature increase (from 100°C to 200°C) the structure did not feature any board-like formations, which were replaced by skeletal formations. We used the sludge particle from structure in Figure 6b to perform, after deep etching, the so-called mapping using an electron microscope. Mapping shows the layout of individual elements in the structure and in the investigated phase. The sludge particle mapping results can be seen in Figure 7. As could be anticipated based on theoretical knowledge, the sludge particle in Figure 7 consisted mainly of chromium and iron, whereas aluminium and silicon were distributed mostly in the matrix. However, low manganese content was detected by mapping only partially.

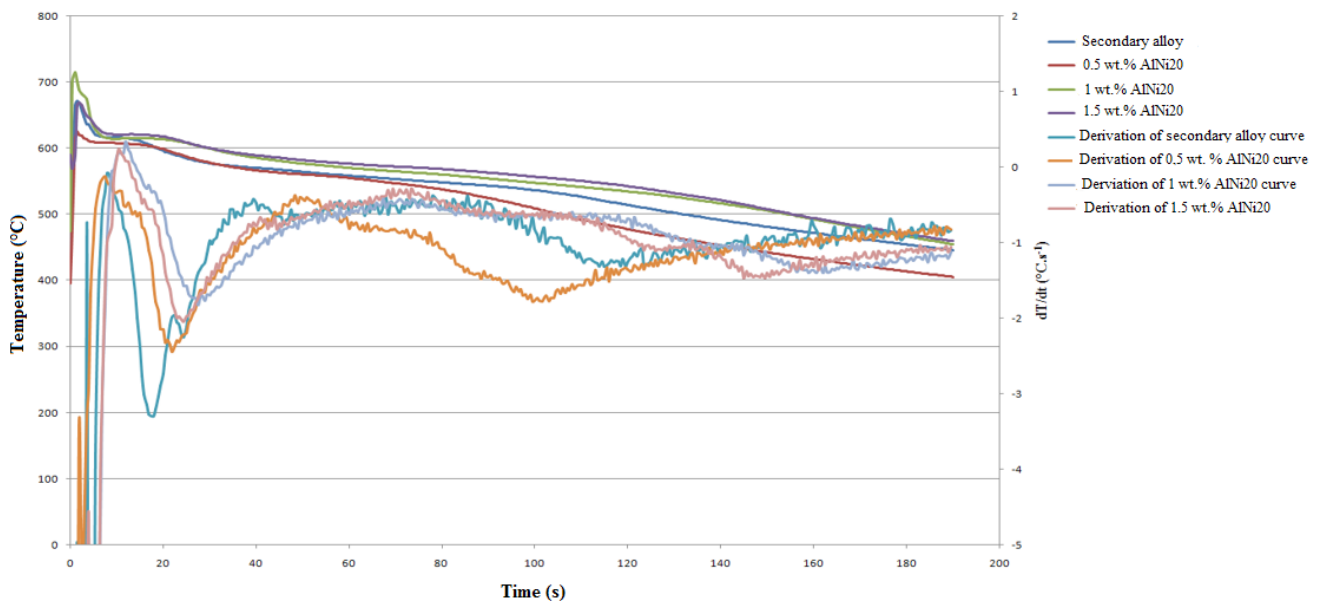


Fig. 3. Record of thermal analysis of AlSi7Mg0.3 secondary alloy after adding AlNi20 master alloy

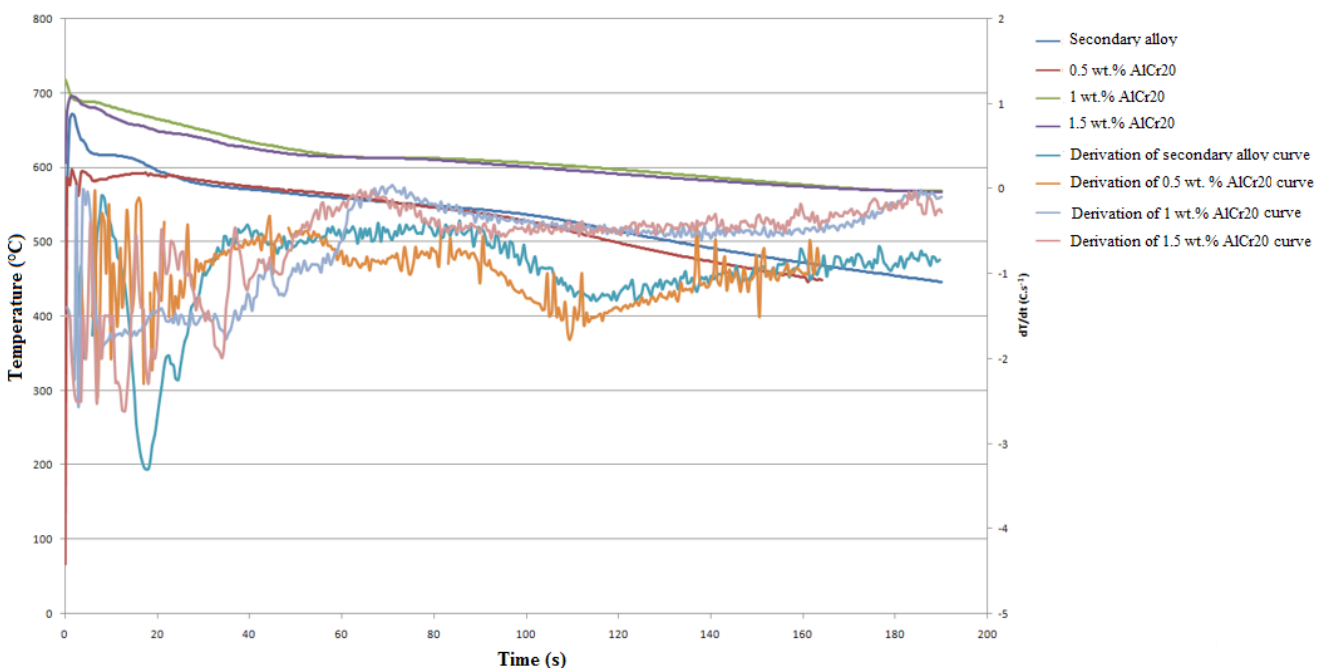
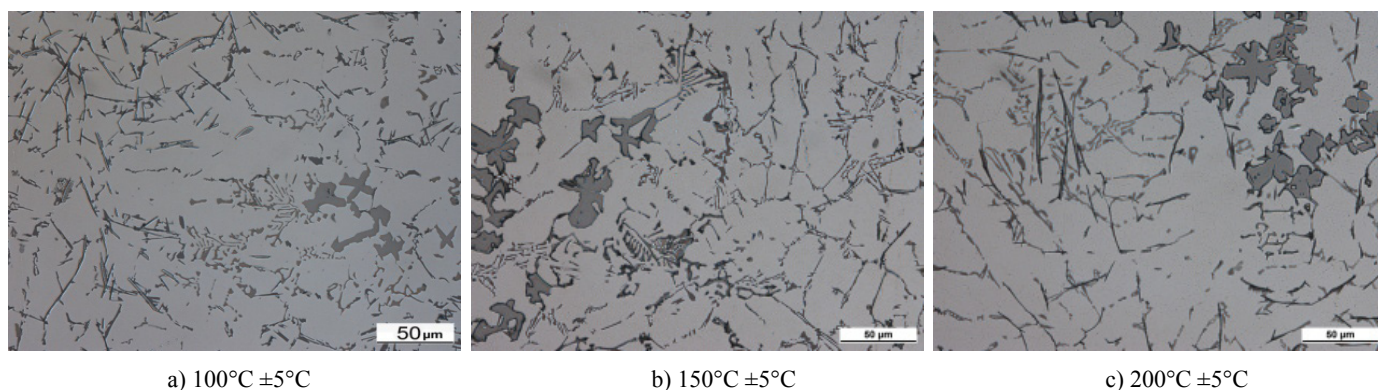


Fig. 4. Record of thermal analysis of AlSi7Mg0.3 secondary alloy after adding AlCr20 master alloy

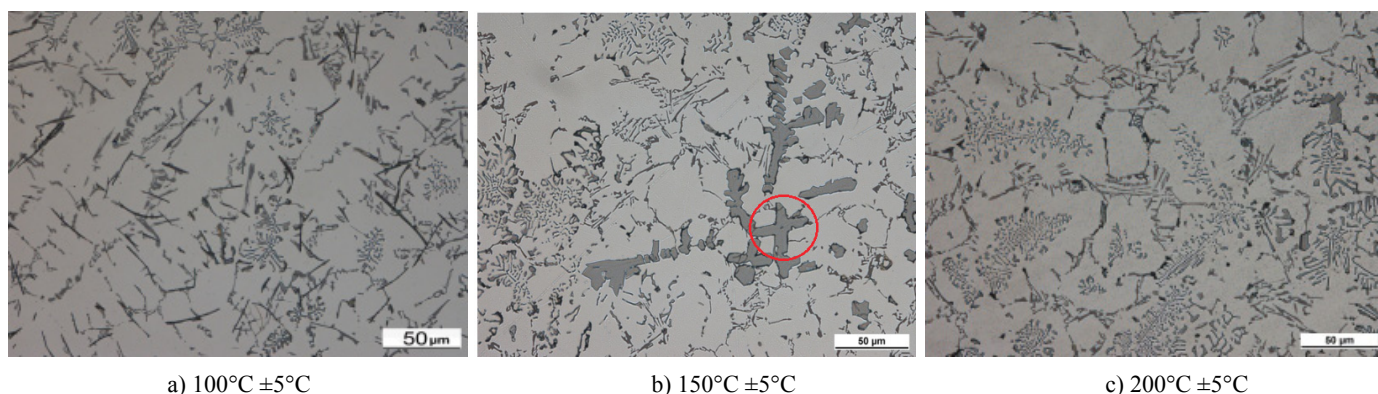


a) 100°C ±5°C

b) 150°C ±5°C

c) 200°C ±5°C

Fig. 5. Microstructure of AlSi7Mg0.3 secondary alloy with different mould temperatures after adding 0.5 wt. % of AlCr20



a) 100°C ±5°C

b) 150°C ±5°C

c) 200°C ±5°C

Fig. 6. Microstructure of AlSi7Mg0.3 secondary alloy with different mould temperatures after adding 1 wt. % of AlCr20

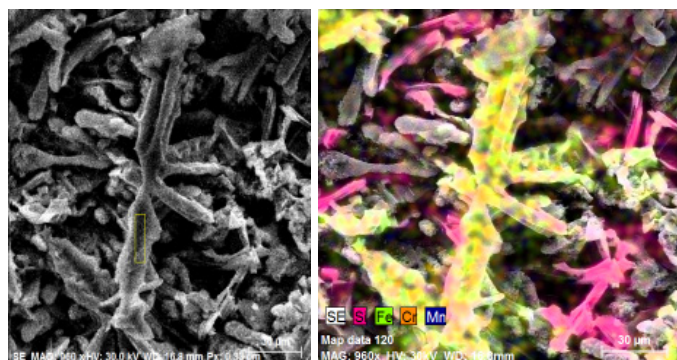


Fig. 7. Mapping of the sludge phase in AlSi7Mg0.3 secondary alloy

The impact of the mould preheating after adding 1.5 wt. % of AlCr20 can be seen in Figure 8. Figure 8 clearly shows that increased mould temperatures result in the occurrence in the structure of sludge particle clusters and phases in the shape of “Chinese writing”. Board-like phases did not occur in the amount as in the case of the mould temperature of 100°C ±5°C. The impact of the mould temperature and AlCr20 master alloy (i.e. the corrector) on mechanical properties is shown in Table 2.

As we can see in Table 2, in some cases the mechanical properties of AlSi7Mg0.3 secondary alloy increased compared to the values obtained in casting the alloy into a metal mould with a temperature of 100°C ±5°C. This was particularly the case of the mould preheating temperature of 200°C ±5°C and 1 wt. % addition of AlCr20, when the tensile strength achieved an in-

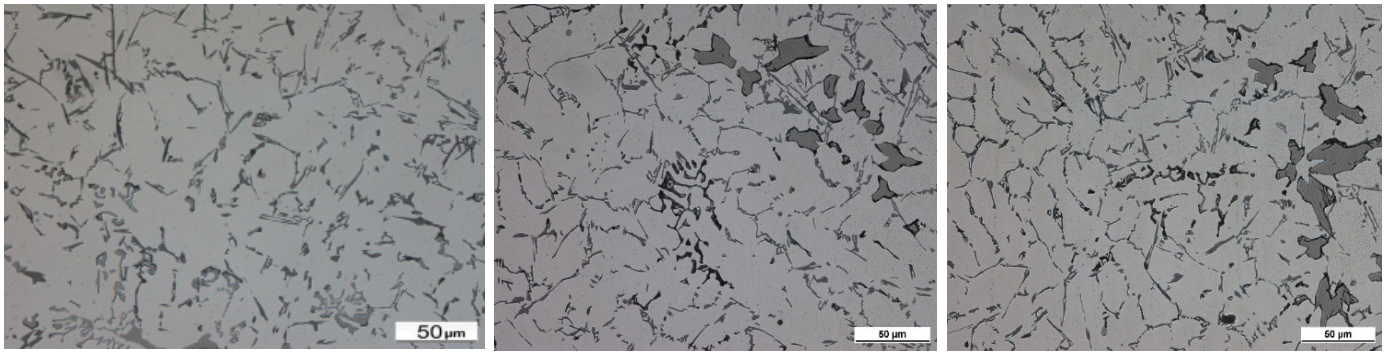
TABLE 2

Mechanical properties of AlSi7Mg0.3 secondary alloy with different mould temperatures with AlCr20 master alloy

Alloy	Corrector AlCr20 (wt. %)	Mould temperature (±5°C)	Tensile strength $R_m$ (MPa)	Ductility $A_5$ (%)	HBS
Secondary AlSi7Mg0.3	No corrector	100	167	0.93	87
		150	149	0.8	83
		200	152	0.78	76
	0.5	100	159	1.02	82
		150	173	1.62	81
		200	167	1.3	77
	1	100	173	1.26	80
		150	179	1.78	77
		200	195	2.51	82
	1.5	100	161	1.11	85
		150	147	0.85	80
		200	141	0.8	78

crease by approximately 14 %, as prescribed by the STN EN 1706 standard for primary alloy, and the ductility level for the first time reached the limit of 2.5% as prescribed by the standard.

Figure 9 shows an image of the microstructure with different mould temperatures after adding 0.5 wt. % of AlNi20. When adding AlNi20 master alloy in the amount of 0.5 wt. % it can be concluded that at increased mould temperatures the  $\beta$ -phase particles did not occur at such a level as in casting into



a) 100°C ± 5°C

b) 150°C ± 5°C

c) 200°C ± 5°C

Fig. 8. Microstructure of AlSi7Mg0.3 secondary alloy with different mould temperatures after adding 1.5 wt. % of AlCr20

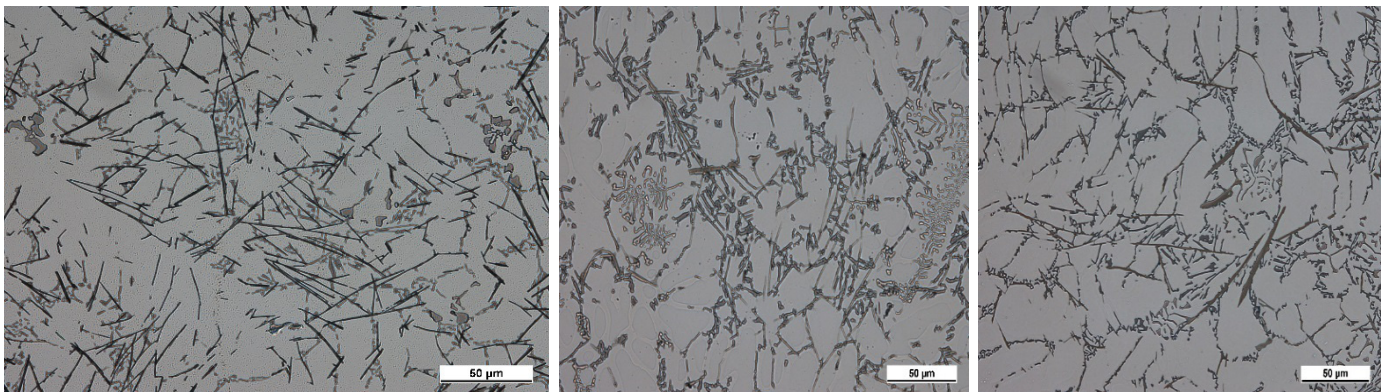
a mould with a temperature of 100°C ± 5°C. Although Figure 9c shows larger particles of board-like formations, these however form rather independent formations than clusters as in the case in Figure 9a. Figure 10 shows images of microstructure after adding 1 wt. % of AlNi20.

After adding 1 wt. % of AlNi20 to AlSi7Mg0.3 secondary alloy we can still observe relatively long particles of  $\beta$ -phase in the structures. A smaller difference was achieved in the case of the mould preheated to 100°C ± 5°C, where board-like formations as well as skeletal formations were excreted in the structure. Figure 11 shows images of microstructures after adding 1.5 wt. % of AlNi20 to AlSi7Mg0.3 secondary alloy.

The best effect on the structure in Figure 11 was achieved by preheating the mould to 100°C ± 5°C or 150°C ± 5°C, when the structure did not feature any long particles of  $\beta$ -phase. Table 3 shows the impact of synergistic effect of the mould preheating and adding corrector AlNi20 on the mechanical properties.

### 3. Conclusion and evaluation of results

The greatest impact of the mould temperature was observed mainly in AlSi7Mg0.3 secondary alloy with no added AlCr20 and AlNi20 master alloys. At the mould temperature 100°C ± 5°C

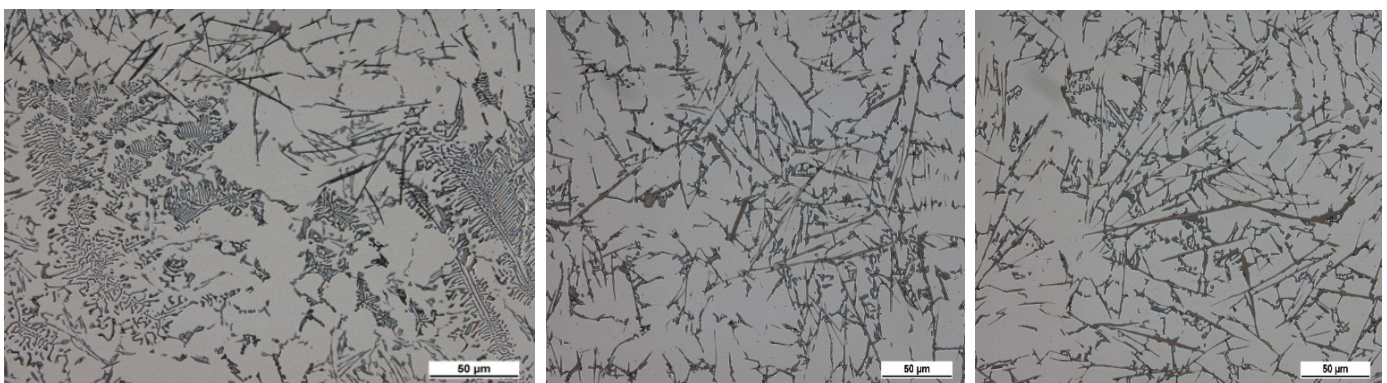


a) 100°C ± 5°C

b) 150°C ± 5°C

c) 200°C ± 5°C

Fig. 9. Microstructure of AlSi7Mg0.3 secondary alloy with different mould temperatures after adding 0.5 wt. % of AlNi20



a) 100°C ± 5°C

b) 150°C ± 5°C

c) 200°C ± 5°C

Fig. 10. Microstructure of AlSi7Mg0.3 secondary alloy with different mould temperatures after adding 1 wt. % of AlNi20

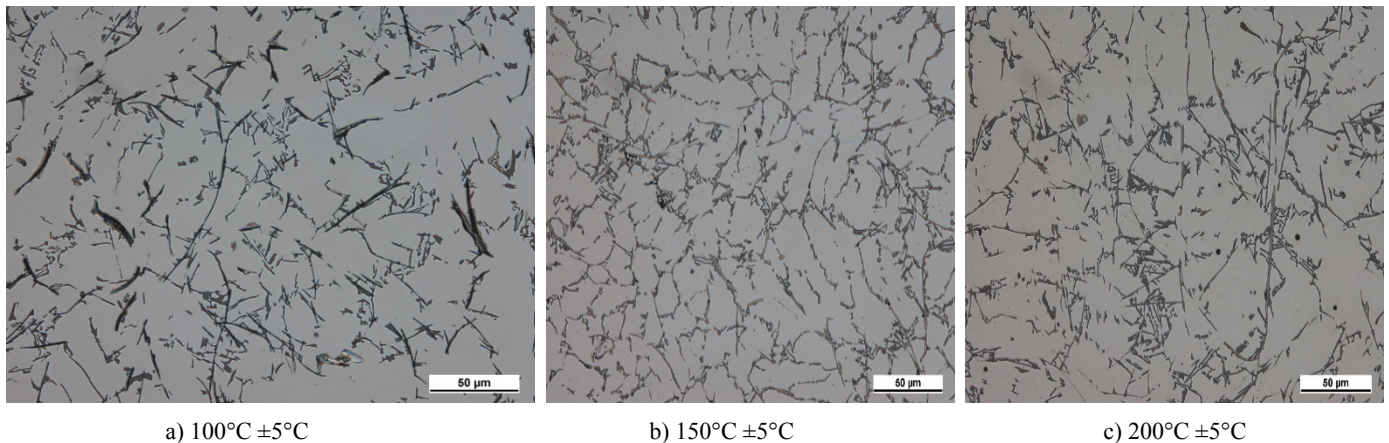


Fig. 11. Microstructure of AlSi7Mg0.3 secondary alloy with different mould temperatures after adding 1.5 wt. % of AlNi20

TABLE 3

Mechanical properties of AlSi7Mg0.3 secondary alloy with different mould temperatures with AlCr20 master alloy

Alloy	Corrector AlNi20 (wt. %)	Mould temperature ( $\pm 5^{\circ}\text{C}$ )	Tensile strength $R_m$ (MPa)	Ductility $A_5$ (%)	HBS
Secondary AlSi7Mg0.3	No corrector	100	167	0.93	87
		150	149	0.8	83
		200	152	0.78	76
	0.5	100	148	0.73	72
		150	150	0.38	78
		200	136	0.49	74
	1	100	160	0.7	72
		150	157	0.6	96
		200	120	0.4	86
	1.5	100	182	1.4	71
		150	168	1	75
		200	140	0.6	83

the structure featured mainly long needles of  $\beta$ -phase, which “vanished” with increasing temperature or changed their shape into skeletal formations or formations in the shape of the so-called “Chinese writing”. With increasing wt. % of correctors the shape of excreted phases changed, but the mould temperature impact on the mechanical properties cannot be unambiguously determined because their values varied with different master alloy contents, and it is thus impossible to determine a clear conclusion regarding the mould temperature at which the best mechanical properties are achieved.

Therefore, a combination of some of the above-mentioned methods seems to be the best way how to eliminate or partially reduce the adverse impact of iron in secondary alloy. The effect of master alloys as correctors was confirmed, when there was a change in the shape of adverse phases. However, it can be concluded that even a possible transformation of adverse phases to more favourable ones paradoxically does not guarantee increased mechanical properties.

Therefore, it can be concluded from the obtained results that, observing the microstructures and mechanical properties,

the best results were achieved in the case of adding 1 wt. % of AlCr20 master alloy, with the ingot mould preheating to  $200^{\circ}\text{C} \pm 5^{\circ}\text{C}$ , when the mechanical properties reached the level of the primary alloy. Board-like formations in this master alloy were of much smaller dimensions and had rounded edges, with minimal occurrence of sludge particles. Using the mould preheating to eliminate negative impacts of iron in Al-Si alloys appears to be the least suitable option, since the mechanical properties values changed discontinuously with different mould temperatures and various correctors.

## REFERENCES

- [1] J.A. Taylor, *Procedia Materials Science* **1**, 19-33 (2012).
- [2] J.A. Taylor, 35th Australian Foundry Institute National Conference, pp. 148-157, Adelaide, South Australia (2004).
- [3] C.M. Dinnis, J.A. Taylor, A.K. Dahle, *Scripta Materialia* **53**, 955-958 (2005).
- [4] X. Cao, J. Campbell **47** (5), 1303-1312 (2006).
- [5] S.S.S. Kumari, R.M. Pillai, T.P.D. Rajan, B.C. Pai, *Material Science and Engineering A*, 460-461 (2007).
- [6] D. Bolibruchová, L. Richtárech, *Manufacturing Technology* **13** (3), 276-281 (2013).
- [7] E. Tillova, M. Chalupova, *Structural analysis of Al-Si cast alloys*, 191. EDIS, Žilina, (2009).
- [8] D. Bolibruchová, M. Zihalova, *Manufacturing technology* **13** (3), 289-296 (2013).
- [9] D. Bolibruchová, M. Brůna, *Manufacturing Technology* **13** (1), (2014).
- [10] R. Pastirčák, *Manufacturing Technology* **14** (3), 397-402 (2015).
- [11] J. Petrik, J. Horvath, *Annals of faculty engineering Hunedoara* **9** (3), 401-405 (2011).
- [12] S. Seifeddine, Literature review, Vilmer project. Jönköping University, 2007.
- [13] M.A. Moustafa, *Journal of Materials Processing Technology* **209** (1), 21-31 (2009).
- [14] E. Tillová, M. Chalupová, L. Hurtalová, M. Bonek, L.A. Dobrzanski, *Journal of Achievements in Materials and Manufacturing Engineering* **47** (1), 19-25 (2011).